Phytotoxic Metabolites Produced by Diaporthella cryptica, the Causal Agent of Hazelnut Branch Canker

JOURNAL OF AGRICULTURAL AND FOOD CHEMISTRY

Article

Cite This: J. Agric. Food Chem. 2018, 66, 3435−3442

pubs.acs.org/JAFC

# Phytotoxic Metabolites Produced by *Diaporthella cryptica*, the Causal Agent of Hazelnut Branch Canker

Alessio Cimmino,*[,†] Paola Nocera,[†] Benedetto Teodoro Linaldeddu,[‡] Marco Masi,[†] Marcin Gorecki,[§] Gennaro Pescitelli,[§] Lucio Montecchio,[‡] Lucia Maddau,[⊥] and Antonio Evidente[†]

[†]Dipartimento Scienze Chimiche, Università di Napoli Federico II, Complesso Universitario Monte S. Angelo, Via Cintia 4, Napoli 80126, Italy

[‡]Dipartimento Territorio e Sistemi Agro-Forestali, Università di Padova, Viale dell'Università 16, Legnaro, Padova 35020, Italy

[§]Dipartimento di Chimica e Chimica Industriale, Università di Pisa, Via Moruzzi, 13, Pisa 56124, Italy

[⊥]Dipartimento di Agraria, Sezione di Patologia Vegetale ed Entomologia, Università degli Studi di Sassari, Viale Italia 39, Sassari 07100, Italy

Supporting Information

**ABSTRACT:** From the culture filtrates of *Diaporthella cryptica*, an emerging hazelnut pathogen, 2-hydroxy-3-phenylpropanoate methyl ester and its 3-(4-hydroxyphenyl) and 3-(1*H*-indol-3-yl) analogues, named crypticins A−C, were isolated together with the well-known tyrosol. Crypticins A−C were identified by spectroscopic (essentially nuclear magnetic resonance and high-resolution electrospray ionization mass spectrometry) methods. The *R* absolute configuration (AC) of crypticin A was determined by comparing its optical rotation and electronic circular dichroism (ECD) spectrum with those of papuline, the methyl ester of (−)(*S*)-phenyllactic acid isolated as the main phytotoxin of *Pseudomonas syringae* pv. *papulans*, responsible for apple blister spot. The ACs of crypticins B and C were determined by time-dependent density functional theory calculations of their ECD spectra. Papuline and the new metabolites herein isolated, except tyrosol, were tested at 1 mg/mL on cork oak, grapevine, hazelnut, and holm oak leaves using the leaf puncture assay. They were also tested on tomato cuttings at 0.5 and 0.05 mg/mL. In the leaf puncture assay, none of the compounds was found to be active. Crypticin C and papuline were active in the tomato cutting assay. Additionally, crypticin C displayed moderate inhibitory effect against *Phytophthora cambivora*.

**KEYWORDS:** *hazelnut branch canker, emerging pathogen, phytotoxins, phenyllactic acid derivatives, TDDFT ECD calculations*



## INTRODUCTION

Hazelnut (*Corylus avellana* L.) is an economically important nut tree historically cultivated along the coasts of the Black Sea in Turkey and in southern Europe.[1] Recently, hazelnut cultivation has widely spread to other countries such as Australia, Azerbaijan, Chile, China, Georgia, Iran, and New Zealand. In all growing areas, hazelnut trees are affected by some severe diseases that can determine heavy economic losses. In particular, branch canker and dieback caused by the fungal species *Anthostoma decipiens*, *Anisogramma anomala*, *Diplodia seriata*, and *Dothiorella coryli* have been recognized as the main biotic factors limiting crop productivity.[2]

Furthermore, a recent study carried out in two grooves located in the center of Sardinia, Italy, revealed the occurrence of several unusual diseases on both young and mature hazelnut trees. In particular, from twigs and branches showing exudates and different types of canker, in addition to several *Botryosphaeriaceae*, a new fungal species was isolated and described as *Diaporthella cryptica*.[2] In the pathogenicity test carried out under controlled conditions, *D. cryptica* proved to be the most aggressive pathogen, causing extensive necrotic lesions, which often girdled the circumference of the logs inoculated.

The genus *Diaporthella* is based on the type species *Diaporthella aristata*[2] and currently encompasses only five species (www.mycobank.org). At the same time to date, detailed morphological features and DNA sequence data are available only for the species *D. corylina* and *D. cryptica*. Because both species have been reported as aggressive pathogens on *Corylus* spp.[2] and no information is available about the bioecology of *D. cryptica*, a study was undertaken to expand the knowledge on the secondary metabolites pattern of this new emerging hazelnut pathogen and identify the virulence factors potentially involved in the pathogenesis process.

## MATERIALS AND METHODS

**General Experimental Procedures.** Optical rotations were measured in $CHCl_3$ or as otherwise reported on a Jasco P-1010 digital polarimeter (Jasco, Tokyo, Japan). Electronic circular dichroism (ECD) spectra were measured with a Jasco J-715 spectropolarimeter in acetonitrile solutions with concentrations ≈1 mM, using quartz cells with different lengths (from 0.01 to 1 cm) to cover the whole wavelength range. $^{1}H$, $^{13}C$ and 2D NMR spectra were recorded at 400 or 500 and 100 or 125 MHz in $CDCl_3$ on Bruker (Karlsruhe, Germany) and Varian (Palo Alto, CA, United States) instruments. The same solvent was also used as internal standard. Carbon multiplicities were determined by distortionless enhancement by polarization transfer (DEPT) spectra.[3] DEPT, correlated spectroscopy (COSY)-

Received: January 15, 2018
Revised: March 12, 2018
Accepted: March 14, 2018
Published: March 14, 2018




DOI: 10.1021/acs.jafc.8b00256
J. Agric. Food Chem. 2018, 66, 3435−3442

45, heteronuclear single quantum coherence (HSQC), heteronuclear multiple bond correlation (HMBC) experiments[3] were performed using Bruker and Varian microprograms. Electrospray ionization mass spectrometry (ESI MS) and liquid chromatography (LC)/MS analyses were performed using the LC/MS TOF system AGILENT (Agilent Technologies, Milan, Italy) 6230B, HPLC 1260 Infinity. The high performance liquid chromatography (HPLC) separations were performed with a Phenomenex (Bologna, Italy) LUNA (C18 (2) 5u 150× 4.6 mm). Analytical and preparative thin-layer chromatography (TLC) were carried out on silica gel (Kieselgel 60, $F_{254}$, 0.25 and 0.5 mm respectively) plates (Merck, Darmstadt, Germany). The spots were visualized by exposure to UV radiation or by spraying first with 10% $H_2SO_4$ in MeOH, and then with 5% phosphomolybdic acid in EtOH, followed by heating at 110 °C for 10 min. Column chromatography was performed using silica gel (Kieselgel 60, 0.063−0.200 mm) (Merck).

**Fungal Strain.** The culture filtrates investigated in this study were obtained from the ex-type culture of *D. cryptica* (CBS 140348) originally isolated from a cankered branch of *C. avellana* L. in Sardinia, Italy.[2] Representative sequences of the isolate CBS 140348 are available in GenBank (ITS: accession number KP205484; EF1-$\alpha$: accession number KP205458).

**Production, Extraction, and Purification of Fungal Metabolites.** *D. cryptica* was grown in 1 L Roux flasks containing 170 mL of Czapek medium (pH 5.7) supplemented with yeast extract (2%). Each flask was seeded with 5 mL of a mycelial suspension and then incubated for 30 days at 25 °C. The fungal cultures, showing phytotoxic activity when tested on tomato cutting as below described, were vacuum filtered through filter paper (Whatman No. 4) to remove the biomass, and the culture filtrates were collected. The culture filtrates (20.3 L) were acidified to pH 4 with 2 N HCl and extracted exhaustively with EtOAc. The combined organic extracts, showing phytotoxic activity in the tomato assay as below reported, were twice washed with distilled water, dried with $Na_2SO_4$, and evaporated under reduced pressure, obtaining brown-red oil residues. The organic extract (2.52 g) was purified by silica gel column chromatography (90 × 4 cm) with $CHCl_3$/*i*-PrOH (9/1, v/v). Seven fractions were collected and pooled on the basis of similar TLC profile, and each group was tested for its phytotoxicity. The residue (70.43 mg) of fraction 2 was further purified by silica gel column chromatography and eluted with *n*-hexane/EtOAc (65/35, v/v), yielding 8 groups of homogeneous fractions. The residue (22.5 mg) of fraction 3 was purified by two successive steps of TLC on silica gel and eluted with petroleum ether/$Me_2CO$ (85/15, v/v) and $CH_2Cl_2$/$Me_2CO$ (98/2, v/v), yielding an amorphous solid, named crypticin A (**1**, $R_f$ 0.8, 8.4 mg, 0.41 mg/L). The residue (90.56 mg) of fraction 3 of the initial column was further purified by silica gel column chromatography and eluted with $CH_2Cl_2$/MeOH (97/3, v/v), affording 8 fractions. The residue (29.10 mg) of the fraction 2 of this latter column was further purified on preparative TLC and eluted with $CHCl_3$/*i*-PrOH (97/3, v/v), yielding an amorphous solid, named crypticin C (**3**, $R_f$ 0.5, 8.5 mg, 0.42 mg/L). The residue (18.57 mg) of fraction 4 was purified by two successive TLC steps using $CHCl_3$/i-PrOH (97/3, v/v) and *n*-hexane/EtOAc (65/35, v/v), affording an amorphous solid, named crypticin B (**2**, $R_f$ 0.2, 6.87 mg, 0.34 mg/L). The residue (174.20 mg) of fraction 4 of the initial column was purified on silica gel column chromatography and eluted with petroleum ether/$Me_2CO$ (7/3, v/v), yielding 9 fractions. The residue (5.27 mg) of fraction 7 was further purified on preparative TLC and eluted with $CHCl_3$/*i*-PrOH (97/3, v/v), yielding another amorphous solid identified, as reported below, as tyrosol (**4**, $R_f$ 0.3, 1.3 mg, 0.06 mg/L).

*Crypticin A (**1**).* $[\alpha]^{25}_D$ +5.2 (c 0.76); IR $\nu_{max}$ 3427, 1739, 1496, 1453, 1215 $cm^{-1}$; UV $\lambda_{max}$ nm (log $\varepsilon$) 273 (2.65); $^1H$ and $^{13}C$ NMR spectra: see Table 1; HRESI MS (+) *m*/*z*: 203.0678 $[C_{10}H_{12}O_3Na$, calcd 203.0684, M + Na$]^+$, 163 $[M + H - H_2O]^+$.

*Crypticin B (**2**).* $[\alpha]^{25}_D$ −4.9 (c 0.62, MeOH); IR $\nu_{max}$ 3339, 1730, 1613, 1515, 1443, 1222 $cm^{-1}$; UV $\lambda_{max}$ nm (log $\varepsilon$) 277 (2.02), 225 (2.00); $^1H$ and $^{13}C$ NMR spectra: see Table 1; HRESI MS (+) *m*/*z*: 415 [2 M + Na$]^+$ 219.0624 $[C_{10}H_{12}O_4Na$, calcd 219.0603, M + Na$]^+$, 179 $[M + H - H_2O]^+$.

**Table 1. $^1H$ and $^{13}C$ NMR Data of Crypticins A and B (1 and 2)[a]**

| | 1 | | | 2 | |
|---|---|---|---|---|---|
| position | δC[b] | δH (*J* in Hz) | HMBC | δC[b] | δH (*J* in Hz) |
| 1 | 174.6 C | | $H_2$-3, H-2 | 174.7 C | |
| 2 | 71.5 CH | 4.48 (1H) m | $H_2$-3 | 71.4 CH | 4.41 (1H) m |
| 3 | 40.6 $CH_2$ | 3.16 (1H) dd (14.0, 4.7) | H-2 | 39.4 $CH_2$ | 3.05 (1H) dd (14.3, 4.5) |
| | | 2.99 (1H) dd (14.0, 6.9) | | | 2.90 (1H) dd (14.3, 6.3) |
| 1′ | 136.3 C | | $H_2$-3, H-2, H-3′,5′ | 128.0 C | |
| 2′, 6′ | 129.5 CH | 7.23 (2H) dd (7.4, 2.0) | H-4′ | 130.7 CH | 7.06 (2H) d (7.6) |
| 3′, 5′ | 128.5 CH | 7.31 (2H) t (7.4) | | 115.4 CH | 6.73 (2H) d (7.6) |
| 4′ | 126.9 CH | 7.26 (1H) td (7.4, 2.0) | H-2′,6′ | 154.5 C | |
| MeO | 52.4 $CH_3$ | 3.80 (3H) s | | 52.4 $CH_3$ | 3.77 (3H) s |
| OH-2 | | 2.74 (1H) br s | | | 2.76 (1H) s |
| OH-4′ | | | | | 5.14 (1H) br s |

[a]The chemical shifts are in δ values (ppm) from TMS. 2D $^1H$, $^1H$ (COSY) $^{13}C$, $^1H$ (HSQC) NMR experiments delineated the correlations of all the protons and the corresponding carbons. [b]Multiplicities were assigned by DEPT spectra.

*Crypticin C (**3**).* $[\alpha]^{25}_D$ −2.6 (c 0.58); IR $\nu_{max}$ 3339, 1730, 1613, 1515, 1443, 1223 $cm^{-1}$; UV $\lambda_{max}$ nm (log $\varepsilon$) 280 (2.16), 220 (2.88); $^1H$ and $^{13}C$ NMR spectra: see Table 2; HRESI MS (+) 242.0794 $[C_{12}H_{13}NO_3Na$ calcd 242.0793, M + Na$]^+$, 220 $[M + H]^+$.

**Table 2. $^1H$ and $^{13}C$ NMR Data of Crypticin C (3)[a]**

| position | δC[b] | δH (*J* in Hz) | HMBC |
|---|---|---|---|
| 1 | 174.8 C | | H-2, $H_2$-3, OMe |
| 2 | 70.8 CH | 4.55 (1H) m | $H_2$-3 |
| 3 | 30.3 $CH_2$ | 3.33 (1H) dd (14.5, 4.8) | H-2 |
| | | 3.22 (1H) dd (14.5, 6.5) | |
| 1′ | | 8.24 (1H) br s | |
| 2′ | 123.1 CH | 7.42 (1H) br s | $H_2$-3 |
| 3′ | 110.2 C | | $H_2$-3, H-2, H-4′, H-2′ |
| 3a′ | 127.3 C | | $H_2$-3, H-2′, H-7′ |
| 4′ | 118.8 CH | 7.77 (1H) d (7.8) | H-6′ |
| 5′ | 119.6 CH | 7.29 (1H) t (7.8) | H-7′ |
| 6′ | 122.2 CH | 7.34 (1H) t (7.8) | H-4′ |
| 7′ | 111.2 CH | 7.51 (1H) d (7.8) | H-5′ |
| 7a′ | 110.1 C | | H-4′, H-2′, H-6′ |
| MeO | 52.43 $CH_3$ | 3.75 (3H) s | |
| OH-2 | | 2.79 (1H) br s | |
| NH | | 8.42 (1H) br s | |

[a]The chemical shifts are in δ values (ppm) from TMS. 2D $^1H$, $^1H$ (COSY) $^{13}C$, $^1H$ (HSQC) NMR experiments delineated the correlations of all the protons and the corresponding carbons. [b]Multiplicities were assigned by DEPT spectrum.

*2-O-Acetyl of Crypticin C (**6**).* Crypticin C (**3**, 0.5 mg) was acetylated with pyridine (20 μL) and $Ac_2O$ (20 μL) at room temperature overnight. The reaction was stopped by addition of MeOH and the azeotrope, obtained by the addition of benzene, was evaporated by an $N_2$ stream. Derivative **6** had: IR $\nu_{max}$ 1747, 1644, 1602, 1573,1234 $cm^{-1}$; UV $\lambda_{max}$ nm (log $\varepsilon$) 272 (3.08); $^1H$ NMR, δ: 8.07 (1H, br s, NH), 7.66 (1H, d, *J* = 8.0 Hz, H-4′), 7.38 (1H, d, *J* =


DOI: 10.1021/acs.jafc.8b00256
J. Agric. Food Chem. 2018, 66, 3435−3442

8.0 Hz, H-7′), 7.22 (1H, t, $J$ = 8.0 Hz, H-6′), 7.16 (1H, t, $J$ = 8.0 Hz, H-5′), 7.11 (1H, br s, H-2′), 5.30 (1H, br t, $J$ = 7.4, H-2), 3.72 (3H, s, OMe), 3.34 (2H, m, $H_2$-3), 2.11 (3H, s, MeCO); ESI MS (+) $m/z$ 300 $[M + K]^+$, 262 $[M + H]^+$.

**Leaf Puncture Assay.** Young cork oak, holm oak, grapevines, and hazelnut leaves were utilized for this assay. All compounds, except tyrosol, and the papuline were assayed at 1.0 mg/mL. Compounds were first dissolved in MeOH, and then a stock solution with sterile distilled water was made. A droplet (20 μL) of test solution was applied on the adaxial sides of leaves that had previously been needle punctured. Droplets (20 μL) of MeOH in distilled water (4%) were applied on leaves as control. Each treatment was repeated three times. The leaves were kept in a moistened chamber to prevent the droplets from drying. Leaves were observed daily and scored for symptoms after 7 days. The effect of the toxins on the leaves was observed up to 10 days. Lesions were estimated using APS Assess 2.0 software following the tutorials in the user's manual.[4] The lesion size was expressed in $mm^2$.

**Tomato Cutting Assay.** Tomato cuttings were taken from 21-day old seedlings, and each compound was assayed at 0.05 and 0.5 mg/mL. Cuttings were placed in the test solutions (3 mL) for 72 h and then transferred to distilled water. Symptoms were visually evaluated up to 7 days. MeOH in distilled water (1%) was used as negative control.

**Antifungal Assays.** The crude ethyl acetate extract of *D. cryptica* was preliminarily tested on a panel of different plant pathogens, including seven fungal species (*Alternaria alternata lycopersici*, *A. brassicicola*, *Athelia rolfsii*, *Botrytis cinerea*, *Fusarium avenaceum*, *F. graminearum*, *Lasiodiplodia mediterranea*) and one oomycete (*Phytophthora cambivora*), which have a great impact in both agricultural and natural ecosystems. The sensitivity of all species to the extract was evaluated on potato-dextrose agar and/or carrot agar medium (CA) as inhibition of the mycelial radial growth. Mycelial plugs (6 mm diameter) were cut from the margin of actively growing 4-day-old colonies using a flamed cork borer. One plug was placed in the center of a 9 cm diameter Petri dish with the mycelia in contact with the medium. Then, 20 μL of the test solution at different concentrations (1000, 500, and 100 μg/plug) was applied on the top of each plug. The negative control was obtained by applying 20 μL of MeOH. The positive controls were metalaxyl-M (mefenoxam; p.a. 43.88%; Syngenta) for oomycete and PCNB (pentachloronitrobenzene) for ascomycetes and basidiomycetes. The plates were incubated at 25 °C in the dark until the target fungi used as negative control covered the plate's surface. Colony diameters were measured in two perpendicular directions for all treatments. Each treatment consisted of three replicates, and the experiment was repeated twice. Subsequently, compounds **1**−**3** and papuline were tested for *in vitro* antifungal activity against the pathogens that resulted more sensitive to the fungal extract. These included *P. cambivora* and *A. brassicicola*. All compounds were tested at 200, 100, and 50 μg/plug as reported above.

**Computational Methods.** Molecular mechanics and preliminary density functional theory (DFT) calculations were run with Spartan16 (Wave Function, Inc., Irvine CA, 2017), with standard parameters and convergence criteria. DFT and time-dependent (TD) DFT calculations were run with Gaussian16[5] with default grids and convergence criteria. Conformational searches were run with the Monte Carlo algorithm implemented in Spartan16 using Merck molecular force field (MMFF). The conformers thus obtained were optimized with DFT first at the ωB97X-D/6-31G(d) level and then at the ωB97X-D/6-311+G(d,p) level. Final optimizations were run at the same level, including PCM solvent model for acetonitrile. TDDFT calculations were run with several functionals (CAM-B3LYP, B3LYP, M06, PBE0) and def2-TZVP or aug-cc-pVTZ basis set, including PCM solvent model for acetonitrile. Average ECD spectra were computed by weighting component ECD spectra with Boltzmann factors at 300 K estimated from DFT internal energies. All conformers with population >1% at 300 K were considered; these amounted to 4 conformers for **1**, 8 for **2**, and 7 for **3**. ECD spectra were generated using the program SpecDis,[6] using dipole-length rotational strengths; the difference with dipole-velocity values was negligible in all cases.

## RESULTS AND DISCUSSION

Preliminary extraction experiments of the phytotoxic fungal cultures filtrates were carried out with EtOAc at pH 5.8 (the same of culture filtrates) and pH 4. As the higher phytotoxicity was found testing the organic extract obtained at pH 4, this latter procedure was adopted on large scale. Thus, the corresponding EtOAc organic extract was purified, as reported in details in the Materials and Methods section, yielding three methyl 2-hydroxypropanoate derivatives all as amorphous solid withstanding crystallization, named crypticins A−C, and tyrosol (**1**−**4**, Figure 1). Their purity was ascertained by TLC carried

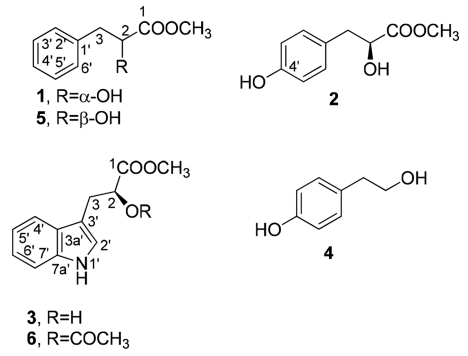


**Figure 1.** Structure of crypticins A−C, tyrosol, papuline (**1**−**5**), and 2-*O*-acetylcrypticin C (**6**).

out on direct and reverse phase and using different solvent mixtures and by $^1$H NMR spectra. The metabolites **1**−**4** were obtained in the yields of 0.41, 0.34, 0.42, and 0.06 mg/L, respectively. Although the structures of **1**−**3** were earlier proposed,[7−10] this is the first time that the suggested structures have been confirmed by means of thorough structure determination using NMR, HR ESIMS, chiroptical, and computational methods, as described below.

Tyrosol (**4**) was identified by comparison of its physical and spectroscopic ($^1$H NMR and ESI MS: see spectra 25 and 26, Supporting Information) data with those previously reported in literature.[11]

The preliminary investigation of $^1$H and $^{13}$C NMR spectra of crypticins A−C showed that they are closely related and contain the same 3-substituted-2-hydroxy propanoate residue.

Crypticin A (**1**) had a molecular formula $C_{10}H_{12}O_3$ as deduced from its HR ESI-MS spectrum and consistent with five hydrogen deficiencies. In particular, its $^1$H NMR and COSY spectra (Table 1)[3] showed the signals of an ABX system appearing as a multiplet at δ 4.48 (H-2) and two double doublets ($J$ = 14.0 and 4.7 Hz and 14.0 and 6.9 Hz) at δ 3.16 and 2.99 ($H_2$-3) together with a sharp and broad singlets of a methoxy and a hydroxy groups (HO-C(2)) at δ 3.80 and 2.74. The signals of a monosubstituted aromatic ring were also observed, as expected, as a double doublet ($J$ = 7.4 and 2.0 Hz) (H-2′,6′), a triplet ($J$ = 7.4 Hz) (H-3′,5′), and a triple doublet ($J$ = 7.4 and 2.0 Hz) (H-4′).[12] These signals were in full agreement with the absorption bands typical for hydroxy, ester carbonyl, and aromatic groups observed in the IR spectrum[13] and the absorption maximum observed in the UV spectrum.[12] The correlations observed in the HSQC spectrum[3] allowed us to assign the signals resonating in the $^{13}$C NMR spectrum (Table 1) at δ 129.5, 128.5, 126.9, 71.5, 52.4, and 40.6 to C-2′,6′, C-3′,5′, C-4′, C-2, MeO, and C-3.[14] In the HMBC spectrum,[3] the couplings of C-1′ at δ 136.1 with the $H_2$-3, H-2,


DOI: 10.1021/acs.jafc.8b00256
J. Agric. Food Chem. 2018, 66, 3435−3442

H-3′, and H-5′ were observed in addition with those expected for the ester carbonyl at $\delta$ 174.6 with $H_2$-3 and H-2. Consequently, the phenyl ring was positioned at C-3 of the methyl ester propanoate, and all the chemical shifts of the protons and the corresponding carbons of **1** were assigned and reported in Table 1. These findings allowed us to formulate crypticin A as methyl 2-hydroxy-3-phenylpropanoate (**1**).

The structure assigned to **1** was confirmed by all the other correlations observed in HMBC spectrum and by the data of its HR ESI MS spectrum. This latter showed the sodium cluster $[M + Na]^+$ at $m/z$ 203.0678 and the ion generated from the protonated molecular ion by loss of $H_2O$ $[M+H-H_2O]^+$ at $m/z$ 163. Thus, crypticin A appeared to be the methyl ester of $\beta$-phenyllactic acid, which was isolated several years ago as the main phytotoxin produced by *Pseudomonas syringae* pv. *papulans*, the causal agent of apple blister spots, and named papuline (**5**, Figure 1).[15] Papuline was also prepared from the commercially available (*S*)-2-hydroxy-3-phenylpropanoic acid.[15] However, when the optical rotation of crypticin A was compared to that of papuline recorded in the same conditions, they showed about the same absolute value but opposite sign. Thus, crypticin A appeared to be the enantiomer of papuline. This was definitely confirmed by comparing their ECD spectra (Figure 2) recorded in the same conditions, which showed a

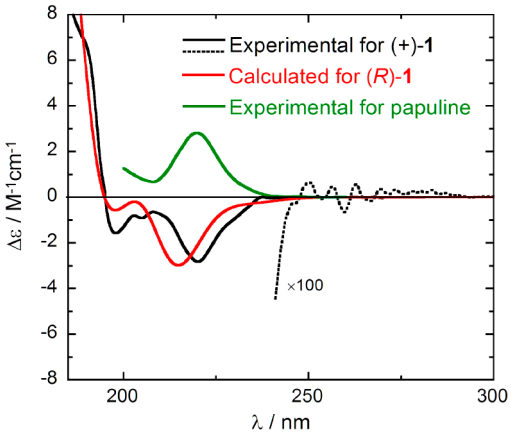


**Figure 2.** Experimental ECD spectra of crypticin A (black lines) and papuline (green line) measured in acetonitrile and calculated ECD spectrum of (*R*)-**1** at B3LYP/def2TZVP/PCM level as Boltzmann average over four structures optimized at the $\omega$B97X-D/6-311+G(d,p)/PCM level. Calculated spectrum plotted as sum of Gaussians with 0.25 eV exponential half-width, scaled by a factor 5.

mirror image relationship, as well as comparing the ECD spectrum of **1** with literature.[16] The ECD spectrum of (+)-(*R*)-**1** was also reproduced by quantum mechanical calculations using a consolidated procedure[17] based on a conformational search with molecular mechanics, geometry optimizations with DFT, and excited state calculations with TDDFT.[18] In the current case, geometry optimizations were run at the $\omega$B97X-D/6-311+G(d,p) level, including a polarizable continuum solvent model (PCM) for acetonitrile, and TDDFT calculations were run with various functionals (B3LYP, CAM-B3LYP, M06, PBE0), the def2TZVP basis set, and PCM for acetonitrile. It must be stressed that simulating the ECD spectrum of simple chiral benzene compounds with good accuracy in the whole wavelength range is far from trivial and requires ad hoc choice of the functional.[17] Moreover, the typical vibronic pattern of the $^1L_b$ band would need vibronic ECD calculations to be reproduced, which is outside the scope of the present manuscript.[17]

In Figure 2, the ECD spectrum calculated on (*R*)-**1** at B3LYP/def2TZVP/PCM level is reported, showing a good agreement with that recorded for crypticin A in the 185−250 nm range. Thus, crypticin A was established as (+)-(*R*)-methyl 2-hydroxy-3-phenylpropanoate (**1**), isolated for the first time as a metabolite of *D. cryptica*, and its complete spectroscopic characterization was reported.

Crypticin A was previously isolated as 3-phenyllactic acid methyl ester from branches and leaves of *Ziziphi jujuba* var. *spinosa*, but no biological activities were reported.[10]

Crypticin B (**2**) had a molecular formula $C_{10}H_{12}O_4$ as deduced from its HR ESIMS spectrum and consistent with five hydrogen deficiencies.

When its $^1H$ and $^{13}C$ NMR spectra (Table 1) were compared to those of **1**, it was obvious that the only difference between crypticin A and B was the presence of a 4-hydroxy phenyl residue as substituent at C-3 of methyl 2-hydroxypropanoate residue of **2** instead of the phenyl group as observed in **1**. In fact, signals of the HC-4′ observed in **1** were absent and that of a OH-C-4′ appeared in the $^{13}C$ NMR spectrum at the typical chemical shift value of $\delta$ 154.5,[14] and a broad singlet of a second hydroxy group resonated in its $^1H$ NMR spectrum at $\delta$ 5.14.

Thus, also on the basis of coupling observed in the COSY, HSQC, and HMBC spectra, the chemical shifts were assigned to all the protons and corresponding carbons (Table 1), and **2** was formulated as methyl 2-hydroxy-3-(4-hydroxyphenyl) propanoate.

This structure was confirmed by the data of its HR ESIMS spectrum which showed the sodiated dimer form $[2 M + Na]^+$ and sodium cluster $[M + Na]^+$ at $m/z$ 415 and 219.0624, respectively. Also, the ion generated from its protonated molecular ion by loss of $H_2O$ $[M+H - H_2O]^+$ was recorded at $m/z$ 179.

Crypticin B appears to be identical to latifolicinin C isolated from *Isodon lophanthiodes* var. *graciliforus*, a plant used in Chinese folk medicine, together with other 12 polyphenols with antioxidant and antibacterial activity.[14] Latifolicinin C was also previously isolated together with seven other metabolites from the roots of *Pulsatilla koreana*, which is endemic in Korea and widely used in traditional medicine for the treatment of several diseases.[8] Furthermore, latifolicinin C was identified by comparison of its spectroscopic and physical data with those previously reported when it was isolated from the fruit of *Cordia latifolia*, a plant used in the folk medicine in the Indo-Pak subcontinent, together with three closely related phenols.[9] Zhou et al.[7] reported an absolute *R* stereochemistry of the chiral C-2 carbon for positive optical rotation, but no data were shown to confirm this attribution. Instead, a recent Korean patent reported negative optical rotation $[\alpha]_D^{25}$ −9.6 for synthetic (*S*)-**2**.[19]

Therefore, there was the necessity to assign the absolute configuration of crypticin B, which was accomplished by the same approach mentioned above for compound **1**. The ECD spectrum of (−)-**2** was recorded in acetonitrile and calculated by the TDDFT method. The calculations run at B3LYP/def2TZVP/PCM level reproduced satisfactorily the experimental spectrum (Figure 3) below 250 nm, while the sign, intensity, and position of the $^1L_b$ band are incorrect. Neither changing the functional (CAM-B3LYP, M06, PBE0) nor increasing the basis set size to aug-cc-pVTZ solved this


DOI: 10.1021/acs.jafc.8b00256
J. Agric. Food Chem. 2018, 66, 3435−3442

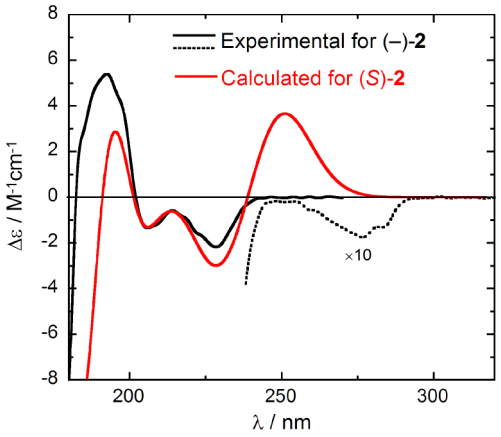


**Figure 3.** Experimental ECD spectrum of crypticin B (black lines) measured in acetonitrile and calculated ECD spectrum of (*S*)-**2** at B3LYP/def2TZVP/PCM level as Boltzmann average over eight structures optimized at ωB97X-D/6-311+G(d,p)/PCM level. Calculated spectrum plotted as sum of Gaussians with 0.25 eV exponential half-width, scaled by a factor 2.

inconsistency. Still, the agreement in the high-energy region of the spectrum allowed us to assign the absolute configuration of crypticin B as (−)-(*S*)-**2**. This is the same configuration obtained for the synthetic latifolicinin C.[19] The compound may thus be established as (−)-(*S*)-2-hydroxy-3-(4-hydroxyphenyl)-propanoate. It is noteworthy that co-occurring **1** and **2** have different configuration at the corresponding chirality center, as well as that (+)-(*R*)-**1** and (−)-(*S*)-**2** have ECD bands of the same sign below 240 nm (Figures 2 and 3). This means that an empirical comparison of ECD spectra would lead to assign the wrong configuration of either of the two compounds. This fact should not be surprising because of the different chromophoric systems arising from OH substitution; for example, the ECD spectra of L-phenylalanine and L-tyrosine are notoriously different.[20]

Crypticin C had a molecular formula of $C_{12}H_{13}NO_3$ deduced from its HR ESI MS and consistent with seven hydrogen deficiencies. The comparison of its $^1$H and $^{13}$C NMR spectra (Table 2) with those of **1** showed that, as for **2**, they differed only for the substituent attached to the C-3 of the methyl 2-hydroxy propanoate residue. In fact, the signals of the phenyl residue observed in **1** were absent, and the signals of a 3-substituted indole residue were instead observed. The broad singlet of the NH group resonated at $\delta$ 8.24 together with the signals of protonated indole ring HC-2′, HC-4′, HC-5′, HC-6′, and HC-7′ assigned by the couplings observed in the COSY and HSQC spectra at $\delta$ 7.42 (s)/123.1 (CH), 7.77 (d, $J$ = 7.8 Hz)/118.8 (CH), 7.29 (t, $J$ = 7.8 Hz)/119.6 (CH), 7.34 (t, $J$ = 7.8 Hz)/122.2 (CH), and 7.51 (d, $J$ = 7.8 Hz)/111.2 (CH).[12,14] The indole quaternary carbons were assigned by the couplings observed in the HMBC spectrum (Table 2) between C-3′ with $H_2$-3, H-3, H-4′, and H-2′, C-3a′ with $H_2$-3, H-2′, and H-7′, and C-7a′ with H-2′, H-4′, and H-6′. Thus, the signals at $\delta$ 127.3, 110.2, and 110.1 were assigned to C-3a′, C-3′, and C-7a′, respectively.

These findings allowed us to formulate crypticin C as methyl 2-hydroxy-3-(1*H*-indol-3-yl)-propanoate. This structure was supported by all the other couplings observed in the HMBC spectrum (Table 2) and from the data of its HR ESI MS spectrum. This latter showed the sodium cluster $[M + Na]^+$ and protonated molecular ion $[M + H]^+$ at $m/z$ 242.0794 and 220, respectively.

Furthermore, the 2-*O*-acetyl derivative of crypticin C (**6**, Figure 1) was also prepared by usual acetylation with pyridine and acetic anhydride. The IR spectrum showed the significant absence of hydroxyl group. The $^1$H NMR of **6** differed from that of **3** for the expected downfield shift ($\Delta\delta$ 0.75) of H-2 observed as a broad triplet ($J$ = 7.4 Hz) at $\delta$ 5.30 and for the presence of the singlet at $\delta$ 2.11 due to the acetyl group. Its ESI MS spectrum showed the potassium cluster $[M + K]^+$ and protonated molecular ion $[M + H]^+$ at $m/z$ 300 and 262, respectively.

The reports on compound **3** as a natural and synthetic compound are contradictory about the absolute configuration (see below) therefore this latter was assigned by means of the aforementioned ECD approach. The experimental ECD spectrum of **3** measured in acetonitrile is compared in Figure 4 with that calculated with TDDFT method at the B3LYP/

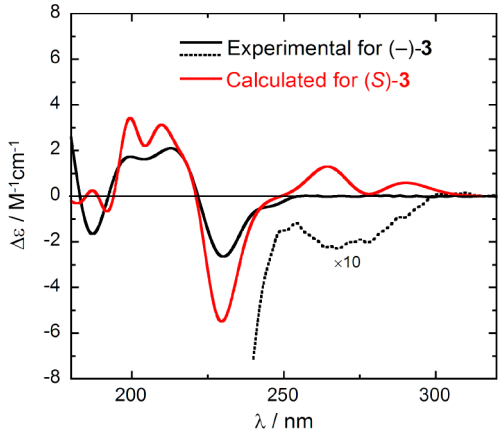


**Figure 4.** Experimental ECD spectrum of crypticin C (black lines) measured in acetonitrile and calculated ECD spectrum of (*S*)-**3** at B3LYP/def2TZVP/PCM level as Boltzmann average over seven structures optimized at ωB97X-D/6-311+G(d,p)/PCM level. Calculated spectrum plotted as sum of Gaussians with 0.25 eV exponential half-width, scaled by a factor 5 and red-shifted by 15 nm.

def2TZVP/PCM level. Once again, the agreement is good enough in the short-wavelength region to assign the absolute configuration as (*S*)-(−)-**3**. In the long-wavelength region, a poorer performance of TDDFT calculations is observed, which was not improved by changing the functional (CAM-B3LYP, M06).

Thus, crypticin C is for first time reported here as a fungal phytotoxin. However, it was previously reported as methyl D-indole-3-lactate produced by the phytopathogenic fungus *Peronophytora litchi*, causing downy blight, a major disease of lychee (*Litchi chinensis* Sonn.).[21] However, Xie et al.[21] did not report any physical or spectroscopic data of D-indole-3-lactate or any biological activity, and only its absolute stereochemistry was described.[21] Successively, it was also isolated from branches and leaves of *Ziziphi jujuba* var. *spinosa* together with the above cited 3-phenyl lactic methyl ester.[10] **3** was also reported as a synthetic intermediate for the total synthesis of several natural compounds such as sattazolin,[22] kurasoins A and B,[23−25] and (neo)oxaline.[26] Furthermore, this compound could be an intermediate of the biosynthetic pathway of indolactic acid (IAA).[27] Interestingly, the above literature is contradictory about the absolute configuration, which is reported to be (*S*)-


DOI: 10.1021/acs.jafc.8b00256
J. Agric. Food Chem. 2018, 66, 3435−3442

(+) by Snyder et al.[22] but (*S*)-(−) by Tsuchiya et al.,[25] Sunazuka et al.,[26] and Zhang et al.[10] despite the fact that all optical rotation data were recorded in chloroform although in different concentrations. In particular, Snyder et al.[22] reported $[\alpha]_D^{25}$ +24.9 (*c* 0.05, chloroform) for (*S*) configuration, which is at odds with our value of $[\alpha]_D^{25}$ −2.60 (*c* 0.58, chloroform) and, more importantly, with our configurational assignment (*S*)-(−) based on ECD results.

In conclusion, the structures of the three cypticins A−C (**1**−**3**) were well supported by their physical and spectral data and absolute configuration assignment. Their chemical and optical purity were based on TLC and NMR experiments and on the comparison of their optical rotations with those reported in literature also deriving from enantioselective syntheses.

Two bioassays were used to investigate the phytotoxic activity of cypticins A−C (**1**−**3**) and papuline. In the leaf-puncture bioassay, the phytotoxicity was evaluated on cork oak, grapevine, hazelnut, and holm oak leaves. None of these compounds was active in this assay at the concentration of 1 mg/mL. In tomato cuttings bioassay, compound **3** and papuline (**5**) were active. Stewing on stem and wilting symptoms were observed at 0.5 and 0.05 mg/mL. None of the other compounds caused any visible symptoms.

The fungal ethyl acetate extract was also screened for antifungal and antioomycete activity in vitro against eight plant pathogens, as reported in the Materials and Methods. These include seven fungal species (*A. alternata lycopersici*, *A. brassicicola*, *A. rolfsii*, *B. cinerea*, *F. avenaceum*, *F. graminearum*, and *L. mediterranea*,) and one oomycete (*P. cambivora*). Among the tested pathogens, *P. cambivora* and *A. brassicicola* were shown to be sensitive to the fungal extract. In particular, the mycelial growth of *P. cambivora* was completely inhibited at 500 μg/plug, whereas *A. brassicicola* was inhibited by 78% at the same concentration. Compounds **1**−**3** and papuline were tested against *P. cambivora* and *A. brassicicola*, the species resulted more sensitive to the fungal extract at 200, 100, and 50 μg/plug. Among them, crypticin C showed moderate activity against *P. cambivora* (52% inhibition) at 200 μg/plug, whereas it weakly inhibited *A. brassicicola* (19% inhibition). No activity was shown by the other compounds at the highest concentration.

These results suggested that the *S* stereochemistry of the C-2 chiral carbon could to be an important feature to induce phytotoxicity as well as the nature of the residue attached to C-3. In fact, papuline and crypticin C, having a different substituent at C-3 but the same *S* stereochemistry at C-2, were phytotoxic, while the other two cypticins A and B, having a similar residue attached to C-3 but opposite stereochemistry at C-2, were inactive.

This study represents the first investigation of phytotoxic secondary metabolites produced by *D. cryptica*, a new emerging hazelnut pathogen in Italy. The EtOAc extract obtained from liquid cultures of *D. cryptica* lead to isolation and characterization of three new derivatives of methyl 2-hydroxypropanoate (cypticins A−C, **1**−**3**) along with tyrosol. Among compounds **1**−**3**, only **3** was found to be active on tomato cuttings. Tyrosol was not tested in this study. However, it is a well-known fungal metabolite produced by several pathogens such as *D. seriata*,[28] *Neofusicoccum australe*,[29] *N. parvum*,[30] *Alternaria tagetica*,[31] *A. brassicicola*,[32] and *Ceratocystis* spp.[33] Its phytotoxic activity on leaves of marigold (*Tagetes erecta* L.), pricklysida (*Sida spinosa* L.), and lamb's quarters (*Chenopodium album* L.) was previously reported.[31,34]

To date, very few studies have investigated the ability of hazelnut pathogens to produce *in vitro* bioactive secondary metabolites. *Pestalotiopsis guepinii*, the causal agent of twig blight on hazelnut in Turkey, has been shown to synthesize lipophilic metabolites, some of which are phytotoxic.[35−37] Additionally, extensive studies on several species of *Botryosphaeriaceae*, some of which were recently reported for the first time as hazelnut pathogens by Linaldeddu et al.,[2] have highlighted the great potential of these fungi to produce *in vitro* a wide range of secondary metabolites, exhibiting various biological activities such as phytotoxic, cytotoxic, and antimicrobial[11,29,38−48] Further and extensive studies are required to better understand the role played by these compounds on the expression of disease symptoms and their potential ecological impact.

## ■ ASSOCIATED CONTENT

### Supporting Information

The Supporting Information is available free of charge on the ACS Publications website at DOI: 10.1021/acs.jafc.8b00256.

Selection of 1D and 2D $^1$H and $^{13}$C NMR, HR ESI MS, IR, and UV spectra (PDF)

## ■ AUTHOR INFORMATION


### Corresponding Author

*Phone: +39 081 2539178; Fax: +39 081 2532126; E-mail: alessio.cimmino@unina.it.

### ORCID

Alessio Cimmino: 0000-0002-1551-4237

Gennaro Pescitelli: 0000-0002-0869-5076

Antonio Evidente: 0000-0001-9110-1656



### Funding

The work was carried out in the frame of Programme STAR 2017 financially supported by Università di Napoli Federico II and Compagania di San Paolo. A.E. is associated with "Istituto di Chimica Biomolecolare del CNR", Pozzuoli, Italy.


### Notes

The authors declare no competing financial interest.

## ■ REFERENCES


(1) Boccacci, P.; Aramini, M.; Valentini, N.; Bacchetta, L.; Rovira, M.; Drogoudi, P.; Silva, A. P.; Solar, A.; Calizzano, F.; Erdoğan, V.; Cristofori, V.; Ciarmiello, L. F.; Contessa, C.; Ferreira, J. J.; Marra, F. P.; Botta, R. Molecular and morphological diversity of on-farm hazelnut (*Corylus avellana* L.) landraces from southern Europe and their role in the origin and diffusion of cultivated germplasm. *Tree Genet. Genomes* **2013**, *9*, 1465−1480.

(2) Linaldeddu, B. T.; Deidda, A.; Scanu, B.; Franceschini, A.; Alves, A.; Abdollahzadeh, J.; Phillips, A. J. L. Phylogeny, morphology and pathogenicity of *Botryosphaeriaceae*, *Diatrypaceae* and *Gnomoniaceae* associated with branch diseases of hazelnut in Sardinia (Italy). *Eur. J. Plant Pathol.* **2016**, *146*, 259−279 (and references therein cited).

(3) Berger, S.; Braun, S. *200 and More Basic NMR Experiments - A Practical Course*, 1st ed.; Wiley-VCH: Weinheim, Germany, 2004.

(4) Lamari, L. *Assess Image Analysis Software for Plant Disease Quantification*; APS Press: St. Paul, MN, United States, 2002.

(5) Frisch, M. J.; Trucks, G. W.; Schlegel, H. B.; Scuseria, G. E.; Robb, M. A.; Cheeseman, J. R.; Scalmani, G.; Barone, V.; Petersson, G. A.; Nakatsuji, H.; Li, X.; Caricato, M.; Marenich, A. V.; Bloino, J.; Janesko, B. G.; Gomperts, R.; Mennucci, B.; Hratchian, H. P.; Ortiz, J. V.; Izmaylov, A. F.; Sonnemberg, J. L.; Williams-Young, D.; Ding, F.; Lipparini, F.; Egidi, F.; Goings, J.; Peng, B.; Petrone, A.; Henderson, T.; Ranasinghe, D.; Zakrzewski, V. G.; Gao, J.; Rega, N.; Zheng, G.;




DOI: 10.1021/acs.jafc.8b00256
J. Agric. Food Chem. 2018, 66, 3435−3442

Liang, W.; Hada, M.; Ehara, M.; Toyota, K.; Fukuda, R.; Hasegawa, J.; Ishida, M.; Nakajima, T.; Honda, Y.; Kitao, O.; Nakai, H.; Vreven, T.; Throssell, K.; Montgomery, J. J. A.; Peralta, J. E.; Ogliaro, F.; Bearpark, M.; Heyd, J. J.; Brothers, E.; Kudin, K. N.; Staroverov, V. N.; Keith, T. A.; Kobayashi, R.; Normand, J.; Raghavachari, K.; Rendell, A.; Burant, J. C.; Iyengar, S. S.; Tomasi, J.; Cossi, M.; Millam, J. M.; Klene, M.; Adamo, C.; Cammi, R.; Ochterski, J. W.; Martin, R. L.; Morokuma, K.; Farkas, O.; Foresman, J. B.; Fox, D. J. *Gaussian 16*, Revision A.03; Gaussian, Inc.: Wallingford CT, 2016.

(6) Bruhn, T.; Schaumlöffel, A.; Hemberger, Y.; Pescitelli, G. *SpecDis*, version 1.70; Berlin, Germany, 2017; https://specdis-software.jimdo.com/ (and references therein cited).

(7) Zhou, W.; Xie, H.; Xu, X.; Liang, Y.; Wei, X. Phenolic constituents from *Isodon lophanthoides* var. *graciliflorus* and their antioxidant and antibacterial activities. *J. Funct. Foods* **2014**, *6*, 492−498.

(8) Cuong, T. D.; Hung, T. M.; Lee, M. K.; Thao, N. T. P.; Jang, H. S.; Min, B. S. Cytotoxic compounds from the roots of *Pulsatilla koreana*. *Nat. Prod. Sci.* **2009**, *15*, 250−255.

(9) Siddiqui, B. S.; Perwaiz, S.; Begum, S. Studies on the chemical constituents of the fruits of *Cordia latifolia*. *Nat. Prod. Res.* **2006**, *20*, 131−137.

(10) Zhang, Q.-Q.; Qi, W.; Wang, W.-N.; Li, M.-X.; Dang, F.; Liu, X.-Q. Isolation and identification of chemical costituents from *Ziziphi spinosae* branch and folium. *J. Shenyang Pharmaceutical University* **2013**, *30*, 917−920 (in Chinese).

(11) Cimmino, A.; Cinelli, T.; Masi, M.; Reveglia, P.; da Silva, M. A.; Mugnai, L.; Michereff, S. J.; Surico, G.; Evidente, A. Phytotoxic lipophilic metabolites produced by grapevine strains of *Lasiodiplodia* species in Brazil. *J. Agric. Food Chem.* **2017**, *65*, 1102−1107 (and literature therein cited).

(12) Pretsch, E.; Buhlmann, P.; Affolter, C. *Structure Determination of Organic Compounds Tables of Spectral Data*, 3rd ed.; Springer-Verlag: Berlin, Germany, 2000; pp 161−243.

(13) Nakanishi, K.; Solomon, P. H. *Infrared Absorption Spectroscopy*, 2nd ed.; Holden Day: Oakland, CA, United States, 1977; pp 17−44.

(14) Breitmaier, E.; Voelter, W. *Carbon-13 NMR Spectroscopy*; VCH: Weinheim, Germany, 1987; pp 183−280.

(15) Evidente, A.; Iacobellis, N. S.; Scopa, A.; Surico, G. Isolation of *β*-phenyllactic acid related compounds from *Pseudomonas syringae*. *Phytochemistry* **1990**, *29*, 1491−1497.

(16) Verbit, L.; Heffron, P. J. Optically active aromatic chromophores—IV: Circular dichroism studies of some open-chain systems. *Tetrahedron* **1968**, *24*, 1231−1236.

(17) Pescitelli, G.; Bruhn, T. Good computational practice in the assignment of absolute configurations by TDDFT calculations of ECD spectra. *Chirality* **2016**, *28*, 466−474 (and references therein cited)..

(18) Srebro-Hooper, M.; Autschbach, J. Calculating natural optical activity of molecules from first principles. *Annu. Rev. Phys. Chem.* **2017**, *68*, 399−420.

(19) Woo, M. H.; Choi, J. S. Composition comprising extract of *Tradescantia spathacea* or compounds isolated there from for preventing or treating metabolic disorder. KR 2016133021, November 22, 2016.

(20) Legrand, M.; Viennet, R. Dichroisme circulaire optique. XV. Etude de quelques acides amines. *Bull. Soc. Chim. Fr.* **1965**, *3*, 679−681.

(21) Xie, H.; Liang, Y.; Xue, J.; Xu, Q.; Jiang, Y.; Wei, X. Secondary metabolites of the phytopathogen *Peronophythora litchii*. *Nat. Prod. Commun.* **2010**, *5*, 245−248.

(22) Snyder, K. M.; Doty, T. S.; Heins, S. P.; DeSouchet, A. L.; Miller, K. A. Asymmetric total synthesis of (+)-sattazolin. *Tetrahedron Lett.* **2013**, *54*, 192−194.

(23) Uchida, R.; Shiomi, K.; Inokoshi, J.; Masuma, R.; Kawakubo, T.; Tanaka, H.; Wai, Y. I.; Omura, S. Kurasoins A and B, new protein farnesyltransferase inhibitors produced by *Paecilomyces* sp. FO-3684. *J. Antibiot.* **1996**, *49*, 932−934.

(24) Christiansen, M. A.; Butler, A. W.; Hill, A. R.; Andrus, M. B. Synthesis of kurasoin B using phase-transfer-catalyzed acylimidazole alkylation. *Synlett* **2009**, *4*, 653−657.

(25) Tsuchiya, S.; Sunazuka, T.; Shirahata, T.; Hirose, T.; Kaji, E.; Omura, S. A new method for efficient coupling of indole and epoxide catalyzed with Yb (OTf) 3, and application to the total synthesis of Kurasoin B. J. *Heterocycles* **2007**, *72*, 91−94.

(26) Sunazuka, T.; Shirahata, T.; Tsuchiya, S.; Hirose, T.; Mori, R.; Harigaya, Y.; Kuwajima, I.; Ōmura, S. A concise stereoselective route to the indoline spiroaminal framework of neoxaline and oxaline. *Org. Lett.* **2005**, *7*, 941−943.

(27) Nutaratat, P.; Srisuk, N.; Arunrattiyakorn, P.; Limtong, S. Indole-3-acetic acid biosynthetic pathways in the basidiomycetous yeast *Rhodosporidium paludigenum*. *Arch. Microbiol.* **2016**, *198*, 429−437.

(28) Venkatasubbaiah, P.; Chilton, W. S. Phytotoxins of *Botryosphaeria obtuse*. *J. Nat. Prod.* **1990**, *53*, 1628−1630.

(29) Andolfi, A.; Maddau, L.; Cimmino, A.; Linaldeddu, B. T.; Franceschini, A.; Serra, S.; Basso, S.; Melck, D.; Evidente, A. Cyclobotryoxide, a phytotoxic metabolite produced by the plurivorous pathogen *Neofusicoccum australe*. *J. Nat. Prod.* **2012**, *75*, 1785−1791.

(30) Evidente, A.; Punzo, B.; Andolfi, A.; Cimmino, A.; Melck, D.; Luque, J. Lipophilic phytotoxins produced by *Neofusicoccum parvum*, a grapevine canker agent. *Phytopathol. Mediterr.* **2010**, *49*, 74−79.

(31) Gamboa-Angulo, M. M.; Garcıá-Sosa, K.; Alejos-González, F.; Escalante-Erosa, F.; Delgado-Lamas, G.; Peña-Rodríguez, L. M. Tagetolone and tagetenolone: two phytotoxic polyketides from *Alternaria tagetica*. *J. Agric. Food Chem.* **2001**, *49*, 1228−1232.

(32) Pedras, C.; Park, M. R. Metabolite diversity in the plant pathogen *Alternaria brassicicola*: factors affecting production of brassicicolin A, depudecin, phomapyrone A and other metabolites. *Mycologia* **2015**, *107*, 1138−1150.

(33) Ayer, W. A.; Browne, L. M.; Feng, M. C.; Orszanska, H.; Saeedi-Ghomi, H. The chemistry of the blue stain fungi. Part 1.Some metabolites of *Ceratocystis* species associated with mountain pine beetle infected lodgepole pine. *Can. J. Chem.* **1986**, *64*, 904−909.

(34) Venkatasubbaiah, P.; Baudoin, A. B. A. M.; Chilton, W. S. Leaf spot of hemp dogbane caused by *Stagonospora apocyni*, and its phytotoxins. *J. Phytopathol.* **1992**, *135*, 309−316.

(35) Karaca, G. H.; Erper, I. First report of *Pestalotiopsis guepinii* causing twig blight on hazelnut and walnut in Turkey. *Plant Pathol.* **2001**, *50*, 415.

(36) Türkkan, M.; Andolfi, A.; Zonno, M. C.; Erper, I.; Perrone, C.; Cimmino, A.; Vurro, M.; Evidente, A. Phytotoxins produced by *Pestalotiopsis guepinii*, the causal agent of hazelnut twig blight. *Phytopathol. Mediterr.* **2011**, *50*, 154−158.

(37) Evidente, A.; Zonno, M. C.; Andolfi, A.; Troise, C.; Cimmino, A.; Vurro, M. Phytotoxic *α*-pyrones produced by *Pestalotiopsis guepinii*, the causal agent of hazelnut twig blight. *J. Antibiot.* **2012**, *65*, 203−206.

(38) Evidente, A.; Masi, M.; Linaldeddu, B. T.; Franceschini, A.; Scanu, B.; Cimmino, A.; Andolfi, A.; Motta, A.; Maddau, L. Afritoxinones A and B, dihydrofuropyran-2-ones produced by *Diplodia africana* the causal agent of branch dieback on *Juniperus phoenicea*. *Phytochemistry* **2012**, *77*, 245−250.

(39) Evidente, A.; Maddau, L.; Spanu, E.; Franceschini, A.; Lazzaroni, S.; Motta, A. Diplopyrone, a new phytotoxic tetrahydropyranpyran-2-one produced by *Diplodia mutila*, a fungus pathogen of cork oak. *J. Nat. Prod.* **2003**, *66*, 313−315.

(40) Masi, M.; Maddau, L.; Linaldeddu, B. T.; Scanu, B.; Evidente, A.; Cimmino, A. Bioactive metabolites from pathogenic and endophytic fungi of forest trees. *Curr. Med. Chem.* **2018**, *25*, 208−252.

(41) Andolfi, A.; Maddau, L.; Cimmino, A.; Linaldeddu, B. T.; Basso, S.; Deidda, A.; Serra, S.; Evidente, A. Lasiojasmonates A−C, three jasmonic acid esters produced by *Lasiodiplodia* sp., a grapevine pathogen. *Phytochemistry* **2014**, *103*, 145−153.

(42) Andolfi, A.; Maddau, L.; Basso, S.; Linaldeddu, B. T.; Cimmino, A.; Scanu, B.; Deidda, A.; Tuzi, A.; Evidente, A. Diplopimarane, a 20-nor-ent-pimarane produced by the oak pathogen *Diplodia quercivora*. *J. Nat. Prod.* **2014**, *77*, 2352−2360.



DOI: 10.1021/acs.jafc.8b00256
*J. Agric. Food Chem.* 2018, 66, 3435−3442

(43) Abou-Mansour, E.; Débieux, J. L.; Ramírez-Suero, M.; Bénard-Gellon, M.; Magnin-Robert, M.; Spagnolo, A.; Chong, J.; Farine, S.; Bertsch, C.; L'Haridon, F.; Serrano, M.; Fontaine, F.; Rego, C.; Larignon, P. Phytotoxic metabolites from *Neofusicoccum parvum*, a pathogen of Botryosphaeria dieback of grapevine. *Phytochemistry* **2015**, *115*, 207−215.
(44) Masi, M.; Maddau, L.; Linaldeddu, B.T.; Cimmino, A.; D'Amico, W.; Scanu, B.; Evidente, M.; Tuzi, A.; Evidente, A. Bioactive secondary metabolites produced by the oak pathogen *Diplodia corticola*. *J. Agric. Food Chem.* **2016**, *64*, 217−225.
(45) Cimmino, A.; Maddau, L.; Masi, M.; Evidente, M.; Linaldeddu, B. T.; Evidente, A. Further secondary metabolites produced by *Diplodia corticola*, a fungal pathogen involved in cork oak decline. *Tetrahedron* **2016**, *72*, 6788−6793.
(46) Evidente, A.; Venturi, V.; Masi, M.; Degrassi, G.; Cimmino, A.; Maddau, L.; Andolfi, A. In vitro antibacterial activity of sphaeropsidins and chemical derivatives toward *Xanthomonas oryzae* pv. *oryzae*, the causal agent of rice bacterial blight. *J. Nat. Prod.* **2011**, *74*, 2520−2525.
(47) Mathieu, V.; Chantôme, A.; Lefranc, F.; Cimmino, A.; Miklos, W.; Paulitschke, V.; Mohr, T.; Maddau, L.; Kornienko, A.; Berger, W.; Vandier, C.; Evidente, A.; Delpire, E.; Kiss, R. Sphaeropsidin A shows promising activity against drug-resistant cancer cells by targeting regulatory volume increase. *Cell. Mol. Life Sci.* **2015**, *72*, 3731−3746.
(48) Ingels, A.; Dinhof, C.; Garg, A. D.; Maddau, L.; Masi, M.; Evidente, A.; Berger, W.; Dejaegher, B.; Mathieu, V. Computed determination of the in vitro optimal chemocombinations of sphaeropsidin A with chemotherapeutic agents to combat melanomas. *Cancer Chemother. Pharmacol.* **2017**, *79*, 971−983.


DOI: 10.1021/acs.jafc.8b00256
*J. Agric. Food Chem.* 2018, 66, 3435−3442